Two Successive Single Crystal Phase Transitions Involving the Coordination Sphere of Antimony in PhSb(dmit), the First Organo-Antimony(III) Dithiolene Complex

Narcis Avarvari,[1a] Eric Faulques,[1b] and Marc Fourmigué*,[1a]

Sciences Moléculaires aux Interfaces, CNRS FRE 2068, and Laboratoire de Physique Cristalline, CNRS UMR 6502, Institut des Matériaux Jean Rouxel, BP 32229, 2 rue de la Houssinière, 44322 Nantes Cedex 3, France

Received December 21, 2000

PhSb(dmit) ($dmit^{2-}$, 4,5-dithiolato-1,3-dithiole-2-thione), the first neutral organo-antimony dithiolene complex, has been synthesized by addition of $PhSbCl_2$ on a suspension of $Na_2(dmit)$. The complex was characterized by spectroscopic (^1H and ^{13}C NMR and IR) methods and elemental analysis. Its crystal structure was determined by X-ray diffraction at room temperature in the monoclinic $P2_1/c$ space group, with $a = 12.580(3)$, $b = 8.9756(18)$, $c = 15.905(3)$ Å, $\beta = 109.06(3)°$, $V = 1697.5(6)$ Å^3, $Z = 4$. A coordinating THF molecule was found in the structure and the coordination geometry around the antimony atom is of distorted pseudopentagonal bipyramid type, if taking into account the Sb···O and secondary Sb···S interactions, as well as the stereochemically active $5s^2$ lone pair. The intermolecular Sb···S and S···S contacts, shorter than the sum of van der Waals radii of corresponding atoms, lead to the formation of a three-dimensional polymeric network in the solid state. A second X-ray diffraction experiment, performed at 85 K, revealed a very similar monoclinic unit cell with the noncentrosymmetrical space group $P2_1$ with $a = 12.613(3)$, $b = 8.9876(18)$, $c = 15.109(3)$ Å, $\beta = 107.01(3)°$, $V = 1637.8(6)$, $Z = 4$. The structural differences with the first one are basically due to the rotation of the THF ligand in the coordination sphere of the antimony center, leading to the loss of every inversion center found at room temperature. A temperature variable X-ray diffraction study on a PhSb(dmit) single-crystal allowed the detection, with a remarkable accuracy, of two successive first-order phase transitions, the first occurring at T = 162.5 K, while the second was observed at T = 182.5 K. Subsequently, a third set of X-ray data was collected at 180 K and the resulting structure (monoclinic, $P2_1/c$, $a = 16.736(3)$, $b = 8.9653(18)$, $c = 33.132(7)$ Å, $\beta = 91.98(3)°$, $V = 4968.2(17)$, $Z = 12$) derives from the two others by a common b axis, a 3-fold cell volume increase, and the presence of only one-third of the inversion centers present at room temperature. A DSC analysis, showing two endothermic peaks at the expected temperatures, confirms the occurrence of the two structural phase transitions, also in agreement with preliminary Raman data.

Introduction

Intermolecular interactions play an important role in the solid state arrangement of many molecules.[2] This is particularly true in the case of chalcogen rich compounds, where the X···X (X = S, Se, Te) van der Waals interactions can lead to the formation of a two- or three-dimensional network in crystals.[3] In this respect the well-known dithiolene transition metal complexes, which experience in many cases remarkable electronic and magnetic properties, are very relevant.[4] For example, the crystal structure of the mixed-valence superconducting salt $[Me_4N][Ni(dmit)_2]_2$ ($dmit^{2-}$ = 4,5-dithiolato-1,3-dithiole-2-thione) consists of stacks of $Ni(dmit)_2$ moieties, with short intermolecular S···S contacts (about 3.49 Å) which ensure the 2D character of the conductor.[5] In all these complexes the dithiolene fragment can be regarded as a "noninnocent" ligand, since the HOMO is essentially a ligand based orbital, hence involved in the redox processes.[6] This feature, combined with the redox activity of the coordinated metallic center, enables the stabilization of the complexes in several oxidation states. In the special case of dmit, apart from its importance as a "noninnocent" ligand, its neutral organic derivatives are also highly interesting since they are, along with the dmid ($dmid^{2-}$ = 4,5-dithiolato-1,3-dithiole-2-one) derivatives, precursors, via homo- or heterocoupling reactions, of tetrathiafulvalenes (TTF), a well-known class of electroactive donor molecules.[7] In this

(1) (a) Sciences Moléculaires aux Interfaces, CNRS FRE 2068. (b) Laboratoire de Physique Cristalline, CNRS UMR 6502.

(2) (a) Desiraju, G. R. *Crystal Engineering, The Design of Organic Solids, Materials Science Monographs, 54*; Elsevier: Amsterdam, 1989. (b) Desiraju, G. R. *Angew. Chem., Int. Ed. Engl.* **1995**, *34*, 2311.

(3) (a) Inokuchi, H.; Imaeda, K.; Enoki, T.; Mori, T.; Maruyama, Y.; Saito, G.; Okada, N.; Yamochi, H.; Seki, K.; Higuchi, Y.; Yasuoka, N. *Nature* **1987**, *329*, 39. (b) Martin, J. D.; Canadell, E.; Becker, J. Y.; Bernstein, J. *Chem. Mater.* **1993**, *5*, 1199. (c) Ellern, A.; Bernstein, J.; Becker, J. Y.; Zamir, S.; Shahal, L.; Cohen, S. *Chem. Mater.* **1994**, *6*, 1378.

(4) (a) Rauchfuss, T. B. *Progr. Inorg. Chem.*, to be published. (b) Müller-Westerhof, U. T.; Vance, B. In *Comprehensive Coordination Chemistry*; Wilkinson, G., Gillard, R. D., McCleverty, J. A., Eds.; Pergamon Press: Oxford, 1987; Vol. 2, p 596. (c) Cassoux, P.; Valade, L.; Kobayashi, H.; Kobayashi, A.; Clark, R. A.; Underhill, A. E. *Coord. Chem. Rev.* **1991**, *91*, 115. (d) Fourmigué, M. *Coord. Chem. Rev.* **1998**, *178*−*180*, 823. (e) Pullen, A. E.; Olk, R.-M. *Coord. Chem. Rev.* **1999**, *188*, 211.

(5) (a) Kobayashi, A.; Kim, H.; Sasaki, Y.; Kato, R.; Kobayashi, H.; Moriyama, S.; Nishio, Y.; Kajita, K.; Sasaki, W. *Chem. Lett.* **1987**, 1819. (b) Kobayashi, A.; Kim, H.; Sasaki, Y.; Moriyama, S.; Nishio, Y.; Kajita, K.; Sasaki, W.; Kato, R.; Kobayashi, H. *Synth. Met.* **1988**, *27*, B339. (c) Kajita, K.; Nishio, Y.; Moriyama, S.; Kato, R.; Kobayashi, H.; Sasaki, W. *Solid State Commun.* **1988**, *65*, 361.

(6) McCleverty, J. A. *Progr. Inorg. Chem.* **1968**, *10*, 49.

(7) (a) Schukat, G.; Richter, A. M.; Fanghänel, E. *Sulfur Reports* **1987**, *7 (3)*, 155. (b) Schukat, G.; Fanghänel, E. *Sulfur Reports* **1993**, *14*, 245. (c) Svenstrup, N.; Becher, J. *Synthesis* **1995**, 215.

10.1021/ic001439v CCC: $20.00
Published on Web 04/27/2001

case, besides the "classical" HOMO−HOMO overlap and S···S van der Waals interactions in the solid-state structure of functionalized TTF or their radical cation salts, other intermolecular interactions, depending on the functional group attached to the TTF fragment, can occur. For example, hydrogen bonds,[8] halogen···halogen[9] or halogen···nitrogen[10] interactions, and fluorine···fluorine segregation interactions[11] have been evidenced within this class of organic donors in the past few years. The thermodynamic balance between all the possible interactions will drive the solid state arrangement of these compounds and, hence, the conduction and magnetic properties. Therefore the availability of appropriate functional dmit and dmid derivatives, precursors of corresponding tetrathiafulvalenes, appears to be crucial. Moreover, the study of the crystal structure of these functional "half-TTFs" could be very interesting, since one can expect the same type of intermolecular interactions in the corresponding TTFs.

In this respect, the antimony(III) atom appeared to us as a very promising candidate to promote solid state interactions because of its stereochemically active $5s^2$ lone pair on one hand and its capacity to exhibit secondary coordination[12] on the other hand. The well-known examples of distibines,[13] where short Sb···Sb intermolecular contacts, responsible for the thermochromic activity,[14] are observed in the crystalline structure, are particularly relevant for the lone pair activity in solid state.

We therefore decided to investigate redox-active cores such as tetrathiafulvalenes or dithiolenes functionalized by antimony(III) fragments in order to take advantage of the possible Sb···Sb and Sb···S intermolecular interactions in conducting or magnetic solids which can be derived from such multifunctional molecules. We describe here the synthesis, characterization, and X-ray crystal structure of PhSb(dmit). This represents the first neutral organometallic antimony(III) dithiolene complex with a Sb−C bond. Indeed, Doidge-Harrison and Wardell et al. described coordination derivatives of Sb(III) such as $[Q]^+[Sb(dmit)_2]^-$ ($Q^+ = NEt_4^+$, 1,4-Dimethylpyridinium),[15] while the few Sb(V) complexes described in the literature are still salts.[16,17]

Unexpectedly, two fully reversible structural phase transitions were observed on single crystals of PhSb(dmit) upon cooling and were analyzed in details by X-ray diffraction, differential scanning calorimetry, and Raman spectroscopy.

Experimental Section

Synthesis. The reaction was carried out under an inert atmosphere of nitrogen by using Schlenk techniques. Nuclear magnetic resonance spectra were recorded on a Bruker ARX 400 spectrometer operating at 400.13 MHz for ^{1}H and 100.62 MHz for ^{13}C. Chemical shifts are expressed in parts per million downfield from external TMS. The following abbreviations are used: s, singlet; d, doublet; t, triplet. Mass spectrometry was performed on an HP 5989A spectrometer in the EI mode, with an ionization energy of 70 eV. Infrared spectroscopy was measured on a FTIR NICOLET 20 SXC spectrometer. Elemental analysis was performed by the "Service d'analyse du CNRS" at Gif/Yvette, France. 4,5-Bis(thiobenzoyl)-1,3-dithiole-2-thione[18] (**1**) and phenyldichlorostibine[19] were prepared according to published procedures.

Preparation of Phenyl-[4,5-dithiolate-2-thione-1,3-dithiolene]-antimony(III) (2). To a suspension of 4,5-bis(thiobenzoyl)-1,3-dithiole-2-thione (**1**) (2.05 g, 5 mmol) in degassed methanol (60 mL) a freshly prepared sodium methanolate (0.23 g Na, 10 mmol, in 15 mL dry methanol) solution was added at room temperature. After 45 min of magnetic stirring the solution became deep red and the formation of dithiolate was complete. Then a solution of phenyldichlorostibine (1.36 g, 5 mmol) in 10 mL methanol was added and a red solid suddenly appeared. The reaction mixture was further stirred for 3 h at room temperature and after this period the precipitate was filtered, washed with methanol, and dissolved in THF. The solution thus obtained was filtered through a short silica gel column, and after removing the solvent under vacuum, **2** was recovered as a red solid. Yield 1.2 g (60%). Suitable crystals for an X-ray diffraction analysis were grown by layering a small volume of hexane onto a THF solution of **2**.

^{1}H NMR (δ, THF-d_8): 7.35 (tt, 1H, ^3J = 1.3 Hz, ^4J = 8.0 Hz, H-*para*), 7.42 (t, 2H, ^3J = 8.0 Hz, H-*meta*), 7.85 (dd, 2H, ^3J = 8.0 Hz, ^4J = 1.3 Hz, H-*ortho*). ^{13}C NMR (δ, THF-d_8): 127.2 (s, 2CH-*meta*), 128.2 (s, CH-*para*), 128.8 (s, C═C), 132.1 (s, 2CH-*ortho*), 147.3 (s, C-*ipso*), 212.6 (s, C═S). IR(KBr, cm^{-1}): 1433 (m, C═C), 1058 (m, C═S), 1018 (s, C═S), 995 (m, C_6H_5), 893 (m, C−S), 728 (m, C_6H_5), 690 (m, C_6H_5), 529 (w, Sb−C ?), 460 (m, C_6H_5). MS (EI) *m*/*z* (ion, rel intensity): 396, 394 (M^+, 80), 350, 352 ($(M - C{=}S)^+$, 10), 198, 200 ($PhSb^+$, 100). Anal. Calcd for $C_9H_5S_5Sb$: C, 27.35; H, 1.28; S, 40.57. Found: C, 27.69; H, 1.19; S, 40.12.

X-ray Crystallography. Details about data collection and solution refinement are given in Table 1. We have made the choice to present data collected on the same crystal at room temperature and at 180 K and on a second crystal for the structure at 85 K, to show that the behavior we found was not the result of a crystallization hazard. Both crystals experience the same temperature dependence. Data were collected on a Stoe-IPDS imaging plate system for the three structures, whereas the variable temperature X-ray study was performed on a Enraf-Nonius Mach3 four-circle diffractometer, warming the crystal from 95 to 300 K at a 2 K min^{-1} rate. Both diffractometers operate with a Mo−Kα X-ray tube with a graphite monochromator. The structures were solved (SHELXS) by direct methods and refined (SHELXL-97)[20] by full-matrix least-squares methods. Absorption corrections were made for every structure as indicated in Table 1. Hydrogen atoms were introduced at calculated positions (riding model), included in structure factor calculations, and not refined. All the heavy atoms were refined anisotropically except the C_{13} atom in the structure at 180 K. Because of the agitation, restraints of SAME type, taking the O1 THF molecule

(8) (a) Dolbecq, A.; Guiraden, A.; Fourmigué, M.; Boubekeur, K.; Batail, P.; Rohmer, M.-M.; Bénard, M.; Coulon, C.; Sallé, M.; Blanchard, P. *J. Chem. Soc., Dalton Trans.* **1999**, 1241. (b) Heuzé, K.; Fourmigué, M.; Batail, P.; Canadell, E.; Auban-Senzier, P. *Chem. Eur. J.* **1999**, *5*, 2971. (c) Heuzé, K.; Mézière, C.; Fourmigué, M.; Batail, P.; Coulon, C.; Canadell, E.; Auban-Senzier, P.; Jérome, D. *Chem. Mater.* **2000**, *12*, 1898. (d) Moore, A. J.; Bryce, M. R.; Batsanov, A. S.; Heaton, J. N.; Lehman, C. W.; Howard, J. A. K.; Robertson, N.; Underhill, A. E.; Perepichka, I. F. *J. Mater. Chem.* **1998**, *8*, 1541. (e) Dolbecq, A.; Fourmigué, M.; Krebs, F. C.; Batail, P.; Canadell, E.; Clérac, R.; Coulon, C. *Chem. Eur. J.* **1996**, *2*, 1275.

(9) Gompper, R.; Hock, J.; Polborn, K.; Dormann, E.; Winter, H. *Adv. Mater.* **1995**, *7*, 41.

(10) (a) Imakubo, T.; Sawa, H.; Kato, R.; *J. Chem. Soc., Chem. Commun.* **1995**, 1097. (b) Iyoda, M.; Kuwatani, Y.; Hara, K.; Ogura, E.; Suzuki, H.; Ito, H.; Mori, T. *Chem. Lett.* **1997**, 599.

(11) Dautel, O. J.; Fourmigué, M. *J. Org. Chem.* **2000**, *65*, 6479.

(12) Alcock, N. W. *Adv. Inorg. Chem. Radiochem.* **1972**, *15*, 1.

(13) (a) Ashe, A. J., III; Butler, W.; Diephouse, T. R. *J. Am. Chem. Soc.* **1981**, *103*, 207. (b) Mundt, O.; Riffel, H.; Becker, G.; Simon, A. *Z. Naturforsch.* **1984**, *39b*, 317.

(14) Hughbanks, T.; Hoffmann, R.; Whangbo, M.-H.; Stewart, K. R.; Eisenstein, O.; Canadell, E. *J. Am. Chem. Soc.* **1982**, *104*, 3876.

(15) Doidge-Harrison, S. M. S. V.; Irvine, J. T. S.; Spencer, G. M.; Wardell, J. L.; Wei, M.; Ganis, P.; Valle, G. *Inorg. Chem.* **1995**, *34*, 4581.

(16) (a) Spencer, G. M.; Wardell, J. L.; Aupers, J. H. *Polyhedron* **1996**, *15*, 2701. (b) Howie, R. A.; Low, J. N.; Spencer, G. M.; Wardell, J. L. *Polyhedron* **1997**, *16*, 2563.

(17) In the case of heavy elements of group (14) (Sn(IV) and Pb(IV)), besides the correspondent salts, organo-neutral complexes, of R_2M-(dmit) type, were also reported: (a) Doidge-Harrison, S. M. S. V.; Irvine, J. T. S.; Khan, A.; Spencer, G. M.; Wardell, J. L.; Aupers, J. H. *J. Organomet. Chem.* **1996**, *516*, 199. (b) Doidge-Harrison, S. M. S. V.; Irvine, J. T. S.; Spencer, G. M.; Wardell, J. L.; Ganis, P.; Valle, G.; Tagliavini, G. *Polyhedron* **1996**, *15*, 1807.

(18) Steimecke, G.; Sieler, H.-J.; Kirmse, R.; Hoyer, E. *Phosphorus Sulfur* **1979**, *7*, 49.

(19) Nunn, M.; Sowerby, D. B.; Wesolek, D. M. *J. Organomet. Chem.* **1983**, *251*, C45.

(20) Sheldrick, G. M. *Programs for the Refinement of Crystal Structures*; University of Gottingen: Germany, 1997.

Table 1. Crystallographic Data

	PhSb(dmit), r.t.	PhSb(dmit), 85 K	PhSb(dmit), 180 K
formula	$C_{13}H_{13}OS_5Sb$	$C_{13}H_{13}OS_5Sb$	$C_{13}H_{13}OS_5Sb$
mv	467.28	467.28	467.28
crystal system	monoclinic	monoclinic	monoclinic
space group	$P2_1/c$ (No. 14)	$P2_1$ (No. 4)	$P2_1/c$ (No. 14)
a (Å)	12.580(3)	12.613(3)	16.736(3)
b (Å)	8.9756(18)	8.9876(18)	8.9653(18)
c (Å)	15.905(3)	15.109(3)	33.132(7)
β (deg)	109.06(3)	107.01(3)	91.98(3)
V (Å$^{3)}$	1697.5(6)	1637.8(6)	4968.2(17)
Z	4	4	12
d_{calc}, g cm^{-3}	1.828	1.895	1.874
μ cm^{-1}	22.32	23.13	22.87
T (°C)	20	−188	−93
λ (Å)	0.71073	0.71073	0.71073
$R(F_o)^a$	0.0274	0.0352	0.1029
$R_w(F_o^2)^a$	0.0354	0.0411	0.1190

[a] $R(F_o) = \sum||F_o| - |F_c||/\sum|F_o|$, $wR(F_o^2) = [\sum[w(F_o^2 - F_c^2)^2]/\sum[w(F_o^2)^2]]^{1/2}$.

Scheme 1

1 2

as model, were utilized in the refinement cycles for the O_2 and O_3 THF molecules in the structure at 180 K.

DSC Measurement. Differential scanning calorimetry (DSC) measurement was performed on a SETARAM DSC 121 apparatus on a 28 mg crystalline sample of PhSb(dmit). The solid was laid in an aluminum crucible and cooled by a nitrogen flow at a 5 K min^{-1} rate. The cryostat device allowed the cooling of the sample down to 160 K, which proved to be enough for the observation of both transition phases.

Raman Measurements. A single crystal of PhSb(dmit) was attached in a gas-exchange, continuous flow, nitrogen cooled, shielded microcryostat. In this device, the sample was surrounded by the cool nitrogen gas ensuring optimal thermal equilibrium at all investigated temperatures. Backscattering Raman spectra were collected under a microscope objective ×50 by a triple grating spectrometer with a liquid-nitrogen-cooled charge-coupled device detector from 80 K (±0.5 K) to room temperature. The excitation $h\omega_L = 1.83$ eV (676.4 nm) from a Kr^+ laser was chosen to get an optimal spectral resolution of 0.5 cm^{-1}. The spectra were recorded between 10 and 650 cm^{-1}. Spectrometer drift, a possible source of error in measuring frequencies, was nonexistent since gratings were not rotated between each temperature measurement to allow the same spectral bandwidth on the detector. The laser power on the sample was kept as low as possible (1 mW) and defocused on a probed area of 16 μm^2 to avoid thermal degradation.

Results and Discussion

Synthesis, Characterization, and Room-Temperature Crystal Structure of 2. Deprotection of 4,5-bis(thiobenzoyl)-1,3-dithiole-2-thione (**1**), prepared by reaction of $[Et_4N]_2[Zn(dmit)_2]$ with benzoyl chloride, with 2 equiv of base leads to the formation of Na_2dmit, which is very soluble in methanol. Subsequent fast addition of phenyldichlorostibine allows the precipitation of **2** as a red solid. (Scheme 1)

The choice of $PhSbCl_2$ was based on its easy availability and better stability toward oxidation and hydrolysis than the alkylated derivatives. The addition rate of the stibine in the dithiolate solution is an important factor, since we observed that a slow addition gives much lower yields in **2** and its purification is more problematic because secondary products are formed. We suppose that this behavior relies on the affinity of **2**, once formed, to react with a second equivalent of dithiolate to give a reactive dianionic species from which other secondary products can be generated. Further studies are necessary to clear up this point. After a purification step involving the filtration of a THF solution of **2** through a silicagel column, the recovered product gave satisfactory analyses data. The ^{1}H and ^{13}C NMR spectra show the expected signals for aromatic protons and aromatic and dmit carbons, respectively.[15−17] In the IR spectrum (recorded in the range 400−4000 cm^{-1}), all but one absorption frequency was identified, by comparison with literature data.[15−17,21] We assigned the remaining frequency (ν = 529 cm^{-1}) to a Sb−*ipso*-C vibration, although only little and disparate IR or Raman data concerning $PhSbS_2$ systems in this wavenumber range are available in the literature.[22] More extensive studies deal with stibines of R_3Sb type,[23] but the crude comparison with our system would be hazardous since this Sb−C vibration is very sensitive to the coordination scheme around the Sb center. We also ruled out the hypothesis that this frequency could concern a Sb−S vibration because these ones usually appear at much lower values (below 400 cm^{-1}).[24] The molecular structure of **2** was finally confirmed by a X-ray diffraction analysis. Suitable crystals were grown by addition of little hexane in a THF solution of the complex. We were somewhat limited in the choice of crystallization conditions since **2** is completely insoluble in noncoordinating solvents, such as toluene or methylene chloride. Compound **2** crystallizes in the monoclinic system, space group $P2_1/c$, with one molecule in general position in the unit cell. An ORTEP representation of the molecular structure along with the numbering scheme is shown in Figure 1. Selected bond lengths and bond angles are listed in Table 2 and Table 3, respectively. This structure presents some interesting features that will be discussed in detail. The primary coordination sphere of antimony is formed, as expected, by the *ipso* carbon atom of phenyl and the two anionic sulfur atoms of dmit. If one considers the stereochemically active 5s^2 lone pair, we can propose a distorted pseudotetrahedral coordination geometry for the antimony atom.[25] The latter lies practically in the $S_1C_1C_2S_2$ plane, since the torsion angle around the S_1-S_2 axis has a value of only 6.60°(9). In heteroleptic dithiolene complexes this dihedral angle varies with the oxidation state of

(21) Zorn, H.; Schindlbauer, H.; Hammer, D. *Monatsh. Chem.* **1967**, *98*, 731.
(22) Gupta, R. K.; Rai, A. K.; Mehrotra, R. C.; Jain, V. K.; Hoskins, B. F.; Tiekink, E. R. T. *Inorg. Chem.* **1985**, *24*, 3280.
(23) (a) Clark, R. J. H.; Flint, C. D.; Hempleman, A. J. *Spectrochim. Acta* **1987**, *43A*, 805. (b) Ludwig, C.; Dolny, M.; Götze, H.-J. *Spectrochim. Acta, Part A* **1997**, *53*, 2363.
(24) (a) Gates, P. N.; Powell, P.; Steele, D. *J. Mol. Structure* **1971**, *8*, 477. (b) Brill, T. B.; Campbell, N. C. *Inorg. Chem.* **1973**, *12*, 1884.
(25) Schur, M.; Gruhl, A.; Näther, C.; Jeβ, I.; Bensch, W. *Z. Naturforsch.* **1999**, *54b*, 1524.

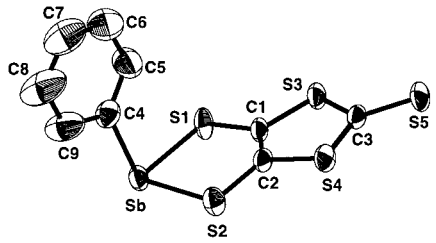

Figure 1. ORTEP view and numbering scheme of PhSb(dmit) at room temperature, with 50% probability displacement ellipsoids. Hydrogen atoms have been omitted.

Table 2. Selected Bond Distances (Å)

	PhSb(dmit), r.t.		
Sb−S_1	2.475(1)	Sb−S_2	2.536(1)
S_1−C_1	1.744(3)	S_2−C_2	1.736(3)
S_3−C_1	1.743(3)	S_4−C_2	1.750(3)
S_3−C_3	1.714(3)	S_4−C_3	1.717(4)
C_1−C_2	1.351(5)	S_5−C_3	1.665(3)
Sb−C_4	2.166(3)	Sb···O	3.015(5)
Sb···$S_{5'}$	3.113(1)	Sb···$S_{5''}$	3.796(2)
Sb···Sb	4.242(1)		
	PhSb(dmit), 85 K		
Sb_1−S_1	2.485(2)	Sb_1−S_2	2.542(2)
Sb_1−C_4	2.166(6)	Sb_1···O_1	2.886(5)
Sb_1···$S_{5'}$	3.070(2)	Sb_1···$S_{10'}$	3.578(2)
Sb_2−S_6	2.532(2)	Sb_2−S_7	2.493(2)
Sb_2−C_{13}	2.181(6)	Sb_2···O_2	2.791(5)
Sb_2···$S_{10'}$	3.129(2)	Sb_2···$S_{5'}$	3.679(2)
Sb_1···Sb_2	4.209(1)		
	PhSb(dmit), 180 K		
Sb_1−S_1	2.541(3)	Sb_1−S_2	2.478(3)
Sb_1−C_4	2.147(14)	Sb_1···O_1	2.982(13)
Sb_1···$S_{5'}$	3.091(3)	Sb_1···$S_{10'}$	3.676(3)
Sb_2−S_6	2.525(3)	Sb_2−S_7	2.495(3)
Sb_2−C_{13}	2.191(10)	Sb_2···O_2	2.849(9)
Sb_2···$S_{10'}$	3.135(3)	Sb_2···$S_{5'}$	3.720(3)
Sb_1···Sb_2	4.224(1)	Sb_3···Sb_3	4.344(3)
Sb_3−S_{11}	2.480(4)	Sb_3−S_{12}	2.527(4)
Sb_3−C_{22}	2.21(3)	Sb_3···O_3	2.969(26)
Sb_3···$S_{15'}$	3.093(5)	Sb_3···$S_{15''}$	3.689(8)

the coordinated center, but in many cases the calculated rotation barrier is quite weak and the observed values are the result of the packing forces in the crystal.[26] The phenyl ring is almost perpendicular on the S_1SbS_2 plane (the dihedral angle value is 87.50°(15)), which is likely due to the stereochemical activity of the lone pair. The coordination of dmit ligand is unsymmetrical, since the Sb−S_2 distance is longer by 0.06 Å than the Sb−S_1 distance but both of them, as well as the Sb−C_4 distance, range within the usual described values.[15,27] Nevertheless, in this configuration, the antimony center is coordinately unsaturated, therefore it engages into secondary bonds in the solid state. This feature is emphasized in Figure 2, which shows the full coordination sphere of the main group element. First of all, we can observe the presence of a THF molecule, in trans to S_1, whose oxygen atom interacts with the antimony atom, in the equatorial plane. The Sb−O distance of 3.015(5) Å is much shorter than the sum of van der Waals radii[28] (about 3.6 Å) and compares, although longer, with the Sb−O distance of 2.85 Å observed in the $[SbI_3(SbMe_3)(THF)]_2$ adduct,[29] but this latter distance was measured at 173 K. A much shorter Sb−O bond of 2.236 Å was found in the stibinidene complex $[(CO)_5Cr]_2Sb(Cl)(THF)$.[30] Our compound thus represents one of the rare Sb(THF) complexes described up to date. Two other secondary interactions, involving the terminal sulfur atoms ($S_{5'}$ and $S_{5''}$) of neighboring dmit moieties, are also observed in the structure of **2**. The shortest one (Sb−$S_{5'}$), located in the equatorial plane determined by S_1, S_2, and O, amounts to 3.113(1) Å; that is about 0.8 Å less than the sum of van der Waals radii of Sb and S. We can consider that this interaction is somewhat stronger than the Sb−O one because the $S_{5'}$ approach in trans to S_2 provokes a lengthening of the Sb−S_2 bond, when compared with the Sb−S_1 one, as noted earlier. The other axial position, trans to C_4, is occupied by $S_{5''}$, at almost a van der Waals distance (3.8 Å), with the axial C_4−Sb−$S_{5''}$ angle at 168.07°(10). Thus, the antimony coordination geometry can be described as a distorted pseudopentagonal bipyramid, with the lone pair located in equatorial position, between $S_{5'}$ and O. Indeed, the $S_{5'}$−Sb−O angle measures 124.77°(11), and a space-filling model of the structure shows some void only between $S_{5'}$ and O. The sum of the equatorial angles about Sb is 360.16° and this atom deviates only by 0.04 Å above the least squares equatorial plane $S_1S_2OS_{5'}$. The Sb···Sb distance within the rectangular frame determined by the two Sb centers and $S_{5'}$ and $S_{5''}$ is 4.24 Å, which equals the sum of van der Waals radii of two Sb atoms. A similar coordination pattern was found in the $[Et_4N][Sb(dmit)_2]$ salt, where the equatorial plane is determined by two anionic sulfur atoms, each from one dmit ligand, and two thiocarbonyl sulfur atoms, responsible for the secondary interactions, from two adjacent $[Sb(dmit)_2]^-$ units.[15] The axial positions are occupied by the two other anionic dmit sulfur atoms and the lone pair is located between the two thiocarbonyl sulfur atoms. The resulting geometry is a distorted pseudopentagonal bipyramid with a distortion which seems to be more pronounced than in our case, although all the coordination sites are occupied by sulfur atoms. Indeed, the sum of equatorial angles about Sb is 369.9° and the axial angle is 158.8°. The existence of two Sb···S=C secondary interactions leads to the formation of polymeric layers of $[Sb(dmit)_2]^-$, separated by cation planes. In the PhSb(dmit) structure described here, the Sb−$S_{5'}$ contacts generate chains running along the *b* direction, which dimerize via the Sb−$S_{5''}$ interactions. Figure 3 shows two parallel infinite dimeric chains, in the *bc* plane, which are separated by phenyl groups. The distance between the aromatic rings is superior to 4.5 Å, so no noticeable $\pi-\pi$ interactions occur. On the other hand the dimeric chains are not isolated from each other, since transversal interchain S_3−$S_{5'}$ interactions are observed. This distance measures 3.55 Å, so it is about 0.05 Å shorter than two times the sulfur van der Waals radius. In Figure 4 one can observe these interchain contacts projected onto the *ac* plane. As a first conclusion we can say that the solid-state structure of PhSb(dmit) is a three-dimensional network formed via Sb···S and S···S secondary interactions, therefore our choice to use an organoantimony fragment coordinated to dmit appears to be justified.

Solid State Phase Transitions: Combined Crystallographic, Calorimetric, and Raman Studies. During a first attempt to measure the X-ray structure of **2** at room temperature, we observed that the crystals lose solvent within several days. Thus the THF coordination to Sb seems to be quite labile and this prompted us to perform low-temperature X-ray data collections on a PhSb(dmit) single crystal in order to check whether temperature dependent structural rearrangements occur.

(26) Domercq, B.; Coulon, C.; Fourmigué, M. *Inorg. Chem.* **2001**, *40*, 371.
(27) Hengstmann, K.-H.; Huber, F.; Preut, H. *Acta Crystallogr.* **1991**, *C47*, 2029.
(28) (a) Bondi, A. *J. Phys. Chem.* **1964**, *68*, 441. (b) Spackman, M. A. *J. Chem. Phys.* **1986**, *85*, 6579.
(29) Breunig, H. J.; Denker, M.; Schulz, R. E.; Lork, E. *Z. Anorg. Allg. Chem.* **1998**, *624*, 81.
(30) Sigwarth, B.; Weber, U.; Zsolnai, L.; Huttner, G. *Chem. Ber.* **1985**, *118*, 3114.

Table 3. Selected Bond Angles (deg)

		PhSb(dmit), r.t.			
S_1-Sb-S_2	86.63(3)	C_4-Sb-S_1	97.30(11)	C_4-Sb-S_2	94.34(10)
$C_4-Sb-S_{5'}$	86.32(10)	C_4-Sb-O	89.10(14)	$C_4-Sb-S_{5''}$	168.07(10)
$S_1-Sb-S_{5'}$	68.75(3)	$S_{5'}-Sb-O$	124.77(11)	$O-Sb-S_2$	80.01(11)
$S_{5''}-Sb-O$	87.56(10)	$S_{5''}-Sb-S_2$	73.79(3)	$S_{5''}-Sb-S_1$	83.54(3)
$S_{5''}-Sb-S_{5'}$	104.97(3)				
		PhSb(dmit), 85 K			
$S_1-Sb_1-S_2$	86.59(6)	$C_4-Sb_1-S_1$	97.39(19)	$C_4-Sb_1-S_2$	91.69(18)
$C_4-Sb_1\cdots S_{5'}$	86.20(18)	$C_4-Sb_1\cdots O_1$	91.69(20)	$C_4-Sb_1\cdots S_{10'}$	167.05(18)
$S_1-Sb_1\cdots S_{5'}$	69.43(6)	$S_{5'}\cdots Sb_1\cdots O_1$	127.87(10)	$O_1\cdots Sb_1-S_2$	76.66(10)
$S_{10'}\cdots Sb_1\cdots O_1$	87.00(10)	$S_{10'}\cdots Sb_1-S_1$	80.46(5)	$S_{10'}-Sb_1-S_2$	75.46(5)
$S_{10'}\cdots Sb_1\cdots S_{5'}$	104.75(5)	$S_6-Sb_2-S_7$	86.63(6)	$C_{13}-Sb_2-S_6$	97.08(17)
$C_{13}-Sb_2-S_7$	97.02(18)	$C_{13}-Sb_2\cdots S_{10'}$	84.44(17)	$C_{13}-Sb_2\cdots O_2$	89.80(20)
$C_{13}-Sb_2\cdots S_{5'}$	174.31(17)	$S_7-Sb_2\cdots S_{10'}$	67.60(6)	$S_{10'}\cdots Sb_2\cdots O_2$	135.86(12)
$O_2\cdots Sb_2-S_6$	70.00(12)	$S_{5'}\cdots Sb_2\cdots O_2$	86.30(10)	$S_{5'}\cdots Sb_2-S_6$	77.69(5)
$S_{5'}\cdots Sb_2-S_7$	85.00(5)	$S_{5'}\cdots Sb_2\cdots S_{10'}$	101.25(4)		
		PhSb(dmit), 180 K			
$S_1-Sb_1-S_2$	86.72(11)	$C_4-Sb_1-S_1$	92.7(4)	$C_4-Sb_1-S_2$	96.8(4)
$C_4-Sb_1\cdots S_{5'}$	86.62(37)	$C_4-Sb_1\cdots O_1$	92.46(47)	$C_4-Sb_1\cdots S_{10'}$	166.95(37)
$S_2-Sb_1\cdots S_{5'}$	68.80(10)	$S_{5'}\cdots Sb_1\cdots O_1$	125.64(23)	$O_1\cdots Sb_1-S_1$	79.15(23)
$S_{10'}\cdots Sb_1\cdots O_1$	85.94(31)	$S_{10'}\cdots Sb_1-S_1$	74.27(9)	$S_{10'}\cdots Sb_1-S_2$	81.97(10)
$S_{10'}\cdots Sb_1\cdots S_{5'}$	104.83(8)	$S_6-Sb_2-S_7$	86.75(10)	$C_{13}-Sb_2-S_6$	95.1(3)
$C_{13}-Sb_2-S_7$	97.6(3)	$C_{13}-Sb_2\cdots S_{10'}$	86.28(29)	$C_{13}-Sb_2\cdots O_2$	88.55(32)
$C_{13}-Sb_2\cdots S_{5'}$	170.78(29)	$S_7-Sb_2\cdots S_{10'}$	67.29(9)	$S_{10'}\cdots Sb_2\cdots O_2$	131.05(24)
$O_2\cdots Sb_2-S_6$	75.03(25)	$S_{5'}\cdots Sb_2\cdots O_2$	85.86(18)	$S_{5'}\cdots Sb_2-S_6$	76.40(9)
$S_{5'}\cdots Sb_2-S_7$	85.53(10)	$S_{5'}\cdots Sb_2\cdots S_{10'}$	102.92(8)	$S_{11}-Sb_3-S_{12}$	86.76(12)
$C_{22}-Sb_3-S_{11}$	96.6(5)	$C_{22}-Sb_3-S_{12}$	94.9(6)	$C_{22}-Sb_3\cdots S_{15'}$	86.77(49)
$C_{22}-Sb_3\cdots O3$	101.26(54)	$C_{22}-Sb_3\cdots S_{15''}$	170.10(60)	$S_{11}-Sb_3\cdots S_{15'}$	68.46(12)
$S_{15'}\cdots Sb_3\cdots O_3$	137.48(30)	$O_3\cdots Sb_3-S_{12}$	66.50(29)	$S_{15''}\cdots Sb_3\cdots O_3$	77.41(30)
$S_{15''}\cdots Sb_3-S_{11}$	80.57(12)	$S_{15''}\cdots Sb_3-S_{12}$	75.49(14)	$S_{15''}\cdots Sb_3\cdots S_{15'}$	100.88(13)

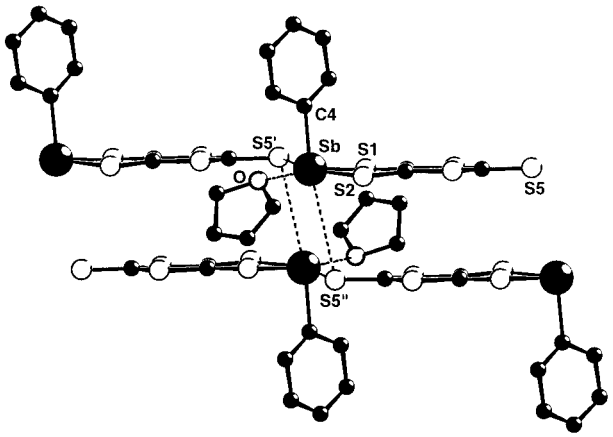

Figure 2. Full coordination sphere of Sb in the structure at room temperature. The Sb···S secondary interactions lead to the formation of centrosymmetric dimers.

Data were collected at 85 K affording a unit cell (Table 1) which differs only slightly (thermal contraction) from that found at room temperature. However the structure was now solved in the monoclinic noncentrosymmetric space group $P2_1$, reflecting the loss, at low temperature, of all inversion centers present at room temperature in the $P2_1/c$ space group. Accordingly, two crystallographically independent PhSb(dmit) molecules are now found in the asymmetric unit. The difference between the two molecules can be easily observed in Figure 5 where the full coordination spheres of the two antimony centers have been depicted. Selected bond lengths and bond angles are listed in Table 2 and Table 3, respectively. Each Sb atom is coordinated, as in the first structure, by one *ipso* carbon atom, two anionic and two thiocarbonyl sulfur atoms, and one oxygen atom. The loss of inversion centers essentially affects the THF molecules which are not equivalent anymore. Indeed, the O_2-THF molecule turned around the Sb_2-O_2 axis during the phase transition while

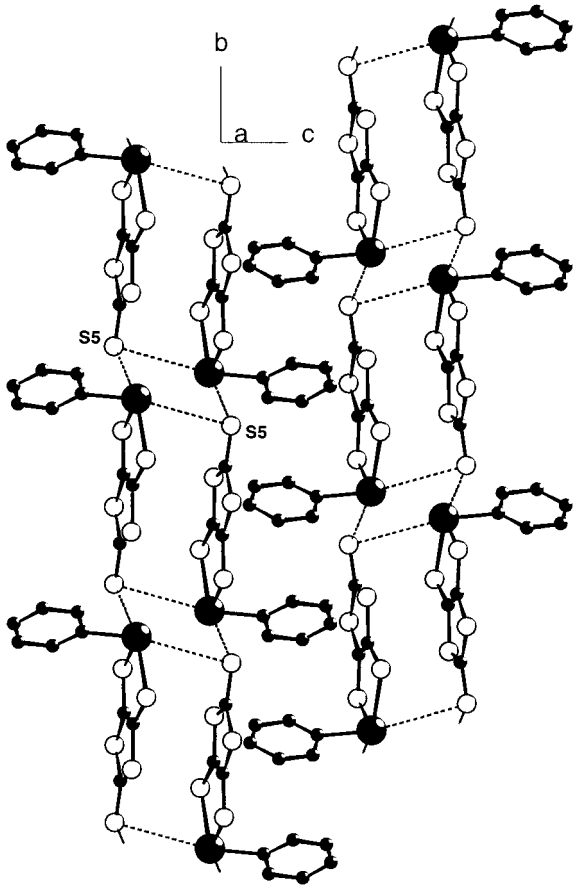

Figure 3. Dimerized infinite chains of PhSb(dmit) running along the *b* direction. THF molecules have been omitted for clarity.

the O_1-THF molecule remained basically in the initial position. To compare the two structures from this point of view we calculated the dihedral angles between THF and the plane

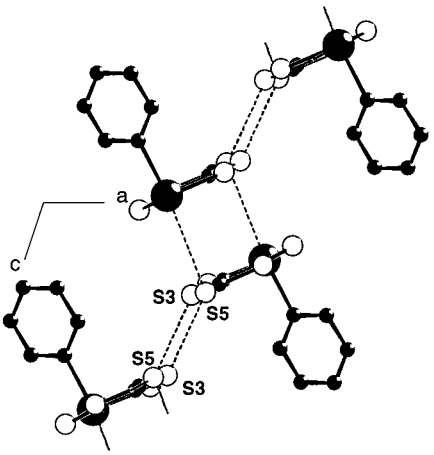

Figure 4. Lateral S···S interactions between dimeric chains in the *ac* plane. THF molecules have been omitted for clarity.

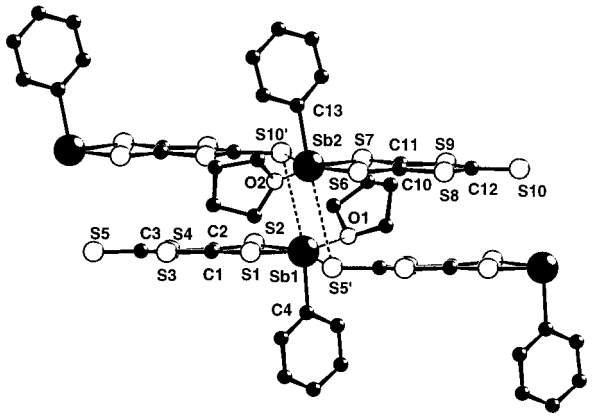

Figure 5. Noncentrosymmetric dimer in the structure at 85 K and numbering scheme for the main atoms of the two independent PhSb(dmit) molecules.

determined by the four equatorial atoms (3S and 1O) around Sb. Thus, for the structure at room temperature this angle has a value of 57.21°(0.35), whereas in the 85 K structure, the angle corresponding to the O_1-THF molecule measures 53.35°(11), comparable with the former value, but the second angle, corresponding to the O_2-THF molecule, measures 70.30°(20). Thus, from a structural point of view, this phase transition mainly involves the rearrangement of half the THF molecules in the coordination sphere of Sb. When comparing the bond lengths and bond angles (Tables 2 and 3) of the two independent molecules based on Sb_1 and Sb_2, the intermolecular distances are also different, especially those involving the connectivity about the antimony atoms. The distortion from a regular pentagonal bipyramid, which includes the $5s^2$ lone pair, is less pronounced in the case of Sb_2 framework for which the folding angle about S_6-S_7 axis is only 2.06°, the sum of the equatorial angles subtended by Sb_2 is 360.09°, the distance from Sb_2 to the equatorial plane is 0.02 Å, and the axial angle $C_{13}-Sb_2-S_5$ is 174.31°(0.17). For the Sb_1 framework the same parameters have the following values: 7.12° (S_1-S_2 axis), 360.55°, −0.05 Å, and 167.05°(0.18) ($C_4-Sb_1-S_{10}$), respectively. One can also remark that the Sb_2-O_2 distance is consistently shorter, by about 0.1 Å, than the Sb_1-O_1 distance, whereas the opposite occurs in the case of Sb···S secondary interactions which are shorter for Sb_1 than for Sb_2. The network formed via secondary interactions consists of chains of Sb_1 in interactions with chains of Sb_2. These mixed dimers interact laterally via S···S van der Waals contacts, as in Figure 4.

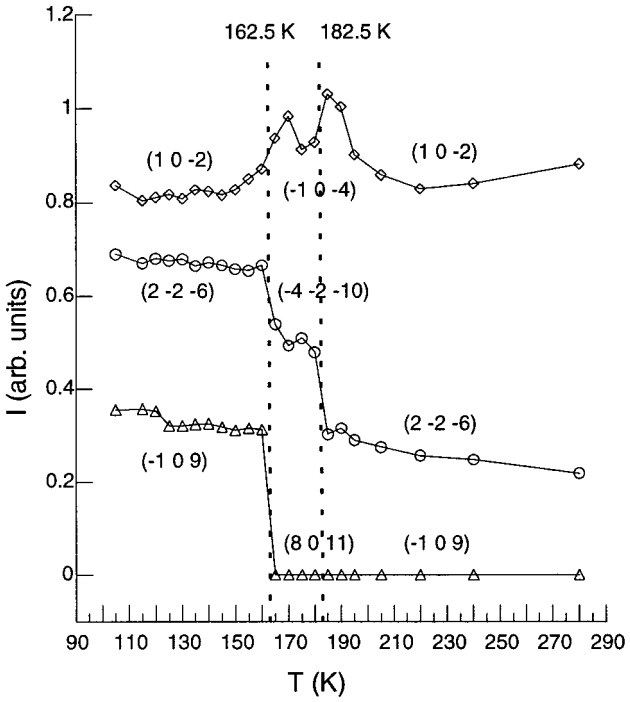

Figure 6. Temperature dependence of the intensities of three reflections. The intensities values have been normalized. The (*hkl*) indexes are given for each reflection in the three different temperature regimes. The two vertical dotted lines indicate the phase transition temperatures.

To get more information about this phase transition, we decided to perform a variable temperature X-ray study on a PhSb(dmit) single crystal. The temperature dependence of the unit cell parameters based on the measurements of twenty five well centered reflections on a four-circle diffractometer, and the temperature dependence of the intensities of those reflections, were investigated between 95 and 300 K. Among the 25 reflections, most of them of general (*hkl*) type with $h,k,l \neq 0$, we also included some of (*h* 0 l) type, with l odd or even. For l even, the (*h* 0 l) reflections are present in both room-temperature $P2_1/c$ and low temperature $P2_1$ space groups but their intensities could display "accidents" at the transition point while with l odd, they should vanish at the transition. To our surprise we did not find one but two fully reversible phase transitions, as observed from the evolution of reflections intensities (Figure 6) and cell parameters (Figure 7), a first one between 160 and 165 K and the second one between 180 and 185 K with a plateau inbetween. Thus, we assume that the first phase transition takes place around 162.5 K and the second around 182.5 K, delimiting a 20 K region with most probably an other solid-state structure which would however conserve the *hkl* reflections observed at low- and room temperature. To determine the crystalline structure in the intermediary phase, a X-ray data collection was performed at 180 K. The 180 K unit cell (Table 1) exhibits a *b* axis common to the low- and room-temperature structures but different *a*, *c*, and β parameters which lead to a 3-fold increase of the unit cell volume. The structure was solved in the monoclinic $P2_1/c$ space group with three crystallographically independent molecules in the asymmetric unit (Figure 8). The final refinement *R* factor has a mediocre value (10.29%) while the same crystal, measured at room temperature, led to a very well refined structure. A measurement at 170 K did not improve the refinement. Most probably, the transition increases the mosaicity and/or induces microscopic twinning, which is then released in the stable low-temperature phase. Besides differences in bond lengths and bond angles,

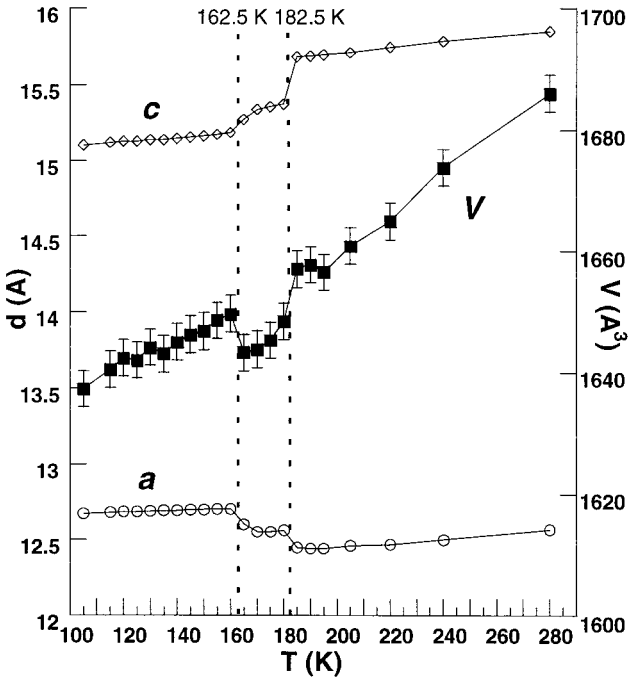

Figure 7. Temperature dependence of the cell parameters *a* and *c* (left *y* axis) and cell volume *V* (right *y* axis). Error bars are negligible for *a* and *c* parameters with respect to the drawing scale. The two vertical dotted lines indicate the phase transition temperatures.

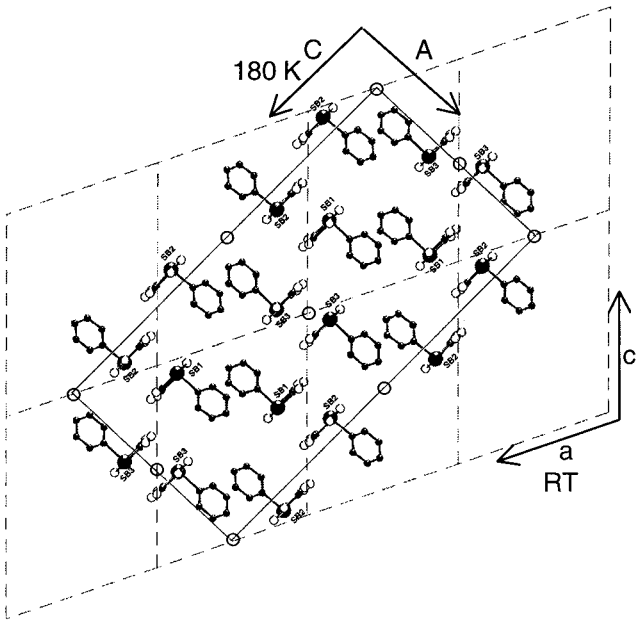

Figure 8. Superposition in the *ac* plane of the crystalline cell at 180 K (full line), filled with the corresponding Sb_1, Sb_2, and Sb_3 PhSb(dmit) molecules, with a range of cells belonging to the structure at room temperature (dashed line). Blank circles represent common inversion centers for both structures. In the structure at room temperature there is only one independent molecule and the number of inversion centers is three times higher than in the structure at 180 K.

the Sb_1, Sb_2, and Sb_3 frameworks have the same geometry as in the two precedent cases. Selected values are shown in Tables 2 and 3, respectively. We will note here only the folding angles about the S···S axis, which refer to the deviation of the antimony center from the dithiolene plane: 7.25°(0.07) for Sb_1 (S_1-S_2), 0.17°(0.04) for Sb_2 (S_6-S_7), and 3.44°(0.07) for Sb_3 ($S_{11}-S_{12}$). These values show once again that the phase transition mainly affects the coordination sphere of antimony, with respect to the

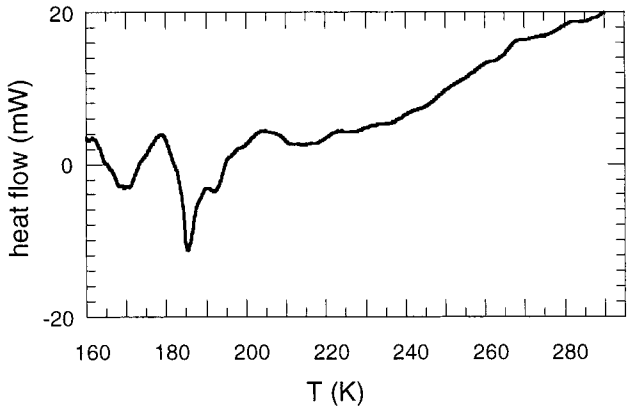

Figure 9. DSC curve obtained by heating a sample of 28 mg of crystalline PhSb(dmit) from 160 K up to room temperature. The two endothermic peaks occur at 168 and 185 K.

THF ligand rearrangement. Indeed, values of 63.75°, 48.81°, and 89.26° were calculated for the dihedral angle between THF and the equatorial plane of Sb_1, Sb_2, and Sb_3, respectively. The polymeric network, resembling the two previously described, is formed by Sb_1 type chains connected with Sb_2 chains via secondary Sb···S interactions, on one hand, and dimerized Sb_3 chains, on the other hand. van der Waals S···S contacts are observed between these infinite dimeric chains.

The existence of the two reversible phase transitions was also ascertained by a DSC[31] measurement on crystalline PhSb(dmit). The curve in Figure 9, representing the temperature dependence of the heat flow when increasing the temperature from 160 K up to room temperature, shows two main endothermic fully reversible peaks, the first one centered at 168 K and the second one at 185 K. The shape of these peaks, as well as the abrupt variations in reflection intensities and cell parameters observed during the X-ray study described above, allow us to assess that both phase transitions are of first order. The associated enthalpy differences, calculated from the peak areas, are 4.10 kJ mol^{-1} for the first transition and 3.30 kJ mol^{-1} for the second one, which is comparable with values described in the literature for other crystalline phase transitions.[32,33] The slight temperature difference between the X-ray and DSC data with regard to the transition points is likely due to the higher temperature variation rate (5 K min^{-1}) in the DSC experience. Information on phase transitions and dynamic processes in solid state can be also obtained by Raman and infrared spectroscopy.[34] With this purpose in mind, we performed Raman measurements on a PhSb(dmit) single crystal at different temperatures and we would like to present here some preliminary results. At the present stage we did not undertake any vibrational analysis in order to characterize the observed modes because this was beyond the scope of this study. Figure 10 shows spectra, obtained at extreme and two intermediate temperatures, plotted in a relevant wavenumber range (0−200 cm^{-1}) where differences between them can be easily observed. Drastic changes versus temperature occur for a couple of line groups, thus proving the evolution of the system upon heating from 80 K up to room temperature. In the lattice modes region (10−100 cm^{-1}), one can observe two lines split at 53 and 59 cm^{-1} below 117 K. At 173 K a single band

(31) Wendlandt, W. Wm. *Thermal Anal.*; Wiley: New York, 1986.
(32) (a) Dunitz, J. D.; Bernstein, J. *Acc. Chem. Res.* **1995**, *28*, 193. (b) Dunitz, J. D. *Acta Crystallogr.* **1995**, *B51*, 619.
(33) Braga, D.; Grepioni, F. *Chem. Soc. Rev.* **2000**, *29*, 229.
(34) Howard, J.; Waddington, T. C. *Advances in Infrared and Raman Spectroscopy*; Hester, R. E., Clark, R. J. H., Eds.; Heyden: London, 1980.

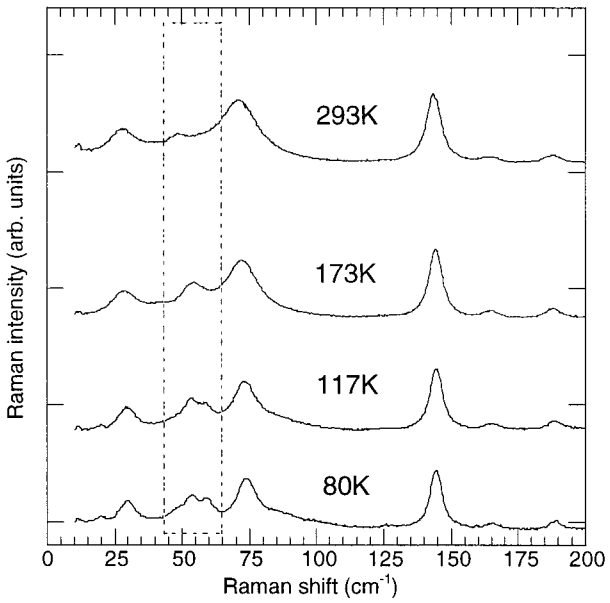

Figure 10. Raman spectra recorded on a PhSb(dmit) single crystal at four different temperatures. The dotted rectangle delimits the line groups where important variations versus temperature were observed.

remains at 54 cm^{-1}, which shifts toward 48 cm^{-1} at room temperature. Therefore the variation of this low-frequency mode is in overall good agreement with the occurrence of three different structural phases within the corresponding thermal regimes.

Relationships between the Three Structures. The three structures described above offer an unique example of two reversible solid-state successive phase transitions on a single crystal. The correspondence between the three structures is illustrated in Figure 8 where the common low- and room-temperature unit cells (in dashed lines) are drawn together with the three time larger 180K unit cell (full line). The *b* axis is the same in both cases, although the origin is shifted. In the reciprocal space, the corresponding relationships write as $\mathbf{a}^*_{RT,LT} = \mathbf{a}^*_{180K} - 2\mathbf{c}^*_{180K}$; $\mathbf{b}^*_{RT,LT} = \mathbf{b}^*_{180K}$; $\mathbf{c}^*_{RT,LT} = \mathbf{a}^*_{180K} + \mathbf{c}^*_{180K}$ and $h_{180K} = h_{RT,LT} + l_{RT,LT}$, $k_{180K} = k_{RT,LT}$ and $l_{180K} = -2h_{RT,LT} + l_{RT,LT}$. As a consequence, the $(-1\ 0\ 9)_{RT,LT}$ reflection, which was present at low temperature (Figure 6), transforms as (8 0 11) at 180K and should then be extinct in the $P2_1/c$ space group at this temperature, as experimentally observed. Actually, because of the $l_{180K} = -2h_{RT,LT} + l_{RT,LT}$ relation, every $(h\ 0\ l)_{RT,LT}$, $l_{RT,LT} = 2n + 1$ extinction of the room-temperature phase is also extinct in the intermediate temperature range. Looking at the evolution of the system from a symmetry point of view, we first note that the 2_1 axis is conserved in the whole temperature range while the inversion centers present at room temperature have fully disappeared at low temperature. In the room-temperature structure, in the $P2_1/c$ space group, there are eight inversion centers per cell and four molecules per cell, so two inversion centers per molecule. On the other hand, in the 180 K structure, there are twelve molecules per cell, which means only 0.66 inversion centers per molecule. As shown in Figure 8, all the inversion centers corresponding to the 180 K structure, represented with blank circles, are preserved, in a ratio of 1:3, from the structure at room temperature. The remaining third of inversion centers completely disappears in the $P2_1$ structure at 85 K. Several crystals were tested and they all shown the same reversible thermal behavior.

The origin and mechanisms of crystalline phase transitions in organic[32] and organometallic[33,35] compounds has been extensively discussed in the literature within the last years. They involve the studies of polymorphism when a given substance exhibits different crystal structures at a given temperature (concomitant polymorphism)[36] but also the situations of reversible single-crystal transformations from one structure into another upon varying the temperature. In organometallic chemistry, those transitions are often associated with the ordering of η^5-C_5H_5 or η^6-C_6H_6 groups. The ferrocene is one of the prototypical examples[32b,37] with a triclinic−monoclinic transition at 242 K while two reversible phase changes are observed in $[(\eta^5\text{-}C_5H_5)_2M][PF_6]$ salts,[38] M = Co, Fe, an order-to-disorder transition above room temperature, and an order-to-order transition at low temperature (213 K with M = Fe). To our knowledge, the two structural transitions observed here in PhSb(dmit)·THF are an unique example of a fully characterized *stepwise* symmetry lowering upon cooling with a successive decrease of the number of inversion centers per molecule and only one-third of them retained in the intermediate regime. The orientation of the THF molecules in the coordination sphere of antimony does not change continuously, but by two first-order transitions which most probably reflect the presence of cooperative intermolecular interactions.[32a] The complex set of short Sb···S and S···S intermolecular contacts found in PhSb(dmit)·THF is likely at the origin of this cooperativity.

Conclusion

The first organo-antimony dithiolene complex, PhSb(dmit), has been synthesized and fully characterized by usual spectroscopic and analytic methods. The careful analysis of its X-ray structure has revealed interesting features, like the inclusion of a THF molecule in the coordination sphere of the antimony, a slightly distorted pseudopentagonal bipyramid around the coordinated center, and secondary intermolecular interactions in the solid. The capacity of the antimony atom to exhibit long range coordination in solid state, in our case with terminal sulfur atoms of neighboring PhSb(dmit) molecules, and the S···S van der Waals contacts led to the formation of a polymeric network in the crystalline state. The two single crystal order-to-order crystalline phase transitions studied by X-ray diffraction, DSC, and partially by Raman spectroscopy demonstrate the rich activity of the antimony atom in the solid state. These results are very encouraging for the purpose of extending our research to other organo-antimony dithiolene complexes, especially by replacing the terminal sulfur atom in dmit moiety with other chalcogen atoms, and to the antimony containing organic donors of TTF type.

Acknowledgment. Financial support from CNRS (Centre National de la Recherche Scientifique) is gratefully acknowledged. The authors thank Stephane Grolleau, from the Laboratoire de Chimie des Solides, Institut des Matériaux Jean Rouxel, Nantes, for the DSC measurement.

Supporting Information Available: Crystallographic data for the three X-ray crystal structures, in CIF format. This material is available free of charge via the Internet at http://pubs.acs.org.

IC001439V

(35) Braga, D. *Chem. Rev.* **1992**, *92*, 633 and references cited herein.
(36) Bernstein, J.; Davey, R. J.; Henck, J.-O. *Angew. Chem., Int. Ed.* **1999**, *38*, 3440.
(37) Dunitz, J. D. In *Organic Chemistry: Its Language and its State of the Art*; Kisakürek, M. V., Ed.; Verlag HCA: Basel, 1993; pp 9−23.
(38) Grepioni, F.; Cojazzi, G.; Draper, S. M.; Sully, N.; Braga, D. *Organometallics* **1998**, *17*, 296.